

## Temperature Driven Reversible Breakdown of Pseudomorphism in Ultrathin Fe/Cu<sub>3</sub>Au Films

F. Bisio,<sup>1,\*</sup> S. Terreni,<sup>1</sup> G. Gonella,<sup>1</sup> L. Floreano,<sup>2</sup> A. Morgante,<sup>2</sup> M. Canepa,<sup>1</sup> and L. Mattera<sup>1</sup>

<sup>1</sup>Unità INFN and CNR-IMEM, Dipartimento di Fisica, Università di Genova, via Dodecaneso 33, I-16146 Genova, Italy

<sup>2</sup>Laboratorio TASC dell'Istituto Nazionale per la Fisica della Materia, Trieste, Italy

(Received 19 January 2004; published 2 September 2004)

We observe that ultrathin Fe/Cu<sub>3</sub>Au(001) films in the 6–13 Å thickness range, beyond the thickness of pseudomorphism breakdown at room temperature, exhibit a temperature dependent structural phase transition in the range  $T_c \approx 345\text{--}380$  K. In the high temperature state the Fe film becomes pseudomorphic, while breakdown of pseudomorphism reversibly occurs as the system is cooled below the transition temperature. The difference between substrate and overlayer thermal expansion coefficient is highlighted as the driving force for the observed transition.

DOI: 10.1103/PhysRevLett.93.106103

PACS numbers: 68.35.-p, 68.55.Jk

The structure of an ultrathin solid film grown on a crystalline substrate generally differs with respect to its bulk counterpart. In the early stages of growth, films typically adopt the substrate periodicity (pseudomorphism) and, after pseudomorphism breakdown, relax towards the unstrained structure. Among the large amount of experimental and theoretical investigations in this field, a large number of studies have aimed to understand the structure of ultrathin iron films epitaxially grown on a variety of substrates [1–9], mainly because of the prediction that Fe films grown with fcc structure could possess intriguing magnetic properties [10–12]. These films, however, are stable only within limited thickness and temperature ranges, factors that become more critical as the lattice mismatch between substrate and bulk Fe equilibrium structure (bcc, lattice constant  $a_{\text{Fe}} = 2.87$  Å) gets larger. In the case of Fe growth on Cu(001) ( $a_{\text{Cu}} = 2.55$  Å), perhaps the most popular example, this “unstable” behavior gives rise to a great sensitivity to fine details of the film preparation procedures [2,4,5], likely related to the coexistence within the same film of a mixture of strained bcc-like and fcc-like phases [6].

Another substrate widely employed for Fe epitaxy is Cu<sub>3</sub>Au(001) [7–9]. Its lattice constant ( $a = 2.65$  Å), being larger than the Cu(001) one, is expected to favor a marginal stability of Fe films grown with fcc structure that might exhibit a critical dependence upon the physical variables governing the state of the system.

In this Letter we report the first observation of a new type of temperature driven structural phase transition. We observe that sweeping the temperature of Fe/Cu<sub>3</sub>Au(001) ultrathin films in the 6–13 Å thickness range across a critical value  $T_c$  reversibly changes their structure so that films are found beyond the pseudomorphism breakdown thickness below  $T_c$  and become fully pseudomorphic at higher temperatures.

Experiments have been performed in two distinct UHV chambers, equipped with facilities for preparation and analysis of thin films. The former apparatus features

He diffraction (HeD) facilities, with a supersonic He beam ( $k_i = 5.87$  Å<sup>-1</sup> and FWHM  $\Delta k/k = 1\%$ ). The latter chamber is equipped with low energy electron diffraction (LEED) instrumentation (Omicron SPECTALEED, home modified for quantitative azimuthal cut measurements), Auger electron spectroscopy (AES), and magneto-optical Kerr effect (MOKE).

The Cu<sub>3</sub>Au surface was treated according to well established procedures [13] until the sample exhibited the typical Cu-Au termination of the so-called  $L1_2$  bulk structure, with sharp diffraction spots, indicative of an ordered surface; Fe films have been deposited evaporating the tip of a high purity wire (99.99%). Film thickness has been determined by monitoring He reflectivity during deposition in the former chamber and by exploiting the presence in the curves of MOKE signal vs deposition time of typical thickness dependent structures [14] and *a posteriori* AES measurements in the latter.

In this work, Fe films of various thickness in the ultrathin limit have been deposited with the substrate held at either low temperature (150 K) or room temperature (RT). Films were subsequently annealed at  $T \approx 400$  K for 10 min, and cooled to room temperature or below (LT state). After thermal treatment, the LEED pattern for films in the 6–11 Å range (150 K growth) and 9–13 Å range (RT growth) reveals the presence of diffraction spots located in pseudomorphic position and sharp superstructure spots symmetrically located around each of them [including (00)], along the (110) and symmetry equivalent directions of the surface primitive cell. The most intense superstructure spots are always the ones located at smaller distance in  $k$  space from the (00) beam, the outer ones being weaker at all electron energies, or even negligible, indicative of the presence of a structure with in-plane spacing larger than the substrate. No indication of second order superstructure peaks is observable along the (110) direction within our experimental accuracy, and line scans measured at several electron energies along the (100) azimuth do not reveal the

presence of corresponding superstructure peaks close to the (00) peak. An electron diffraction line scan measured along the primitive cell (110) direction for low temperature Fe deposition is reported in Fig. 1 (8 Å Fe, electron energy 58.1 eV,  $T = 295$  K). For this pattern, superstructure spots beside the (00) beam, which we term  $\Gamma$ , are clearly visible at  $k_{\parallel}^{\Gamma} = \pm 0.157 \text{ \AA}^{-1}$  (corresponding to a direct space periodicity  $a_{\Gamma} \approx 39 \text{ \AA}$ ). The (11) pseudomorphic peak ( $\pi$ ), located at  $k_{\parallel}^{\pi} = 3.35 \text{ \AA}^{-1}$ , corresponds to the substrate periodicity  $a_{\pi} = 2.65 \text{ \AA}$ . Aside the (11) peak only one superstructure spot that we label  $\gamma$  is seen, located to the left of  $\pi$ . The  $\gamma$  peak, located at  $k_{\parallel}^{\gamma} = 3.20 \text{ \AA}^{-1}$ , corresponds to a structure with real space periodicity  $a_{\gamma} = 2.78 \text{ \AA}$ . Measurements recorded by HeD for this system along both (110) and (100) azimuthal directions substantially confirm LEED measurements concerning the presence and the  $k$ -space position of  $\Gamma$  peaks, while first order diffraction peaks are not detectable due to the sensitivity limit of the apparatus.

Upon increasing the sample temperature, we observe that the  $\pi$  peak intensity  $I_{\pi}$  starts growing at temperature  $T > 340$  K, accompanied by a corresponding decrease of both  $I_{\gamma}$  and  $I_{\Gamma}$  (line scans measured for selected sample temperatures are reported in Fig. 1). The intensity drop of the  $\gamma$  and  $\Gamma$  peaks is accompanied by a shift of their positions;  $k_{\parallel}^{\Gamma}$  increases from  $k_{\parallel}^{\Gamma}(\text{LT}) = 0.157 \text{ \AA}^{-1}$  at LT, to  $k_{\parallel}^{\Gamma}(\text{HT}) \approx 0.18 \text{ \AA}^{-1}$  at  $T \approx 390$  K, while  $k_{\parallel}^{\gamma}$  correspondingly decreases from  $k_{\parallel}^{\gamma}(\text{LT}) = 3.20 \text{ \AA}^{-1}$  to  $k_{\parallel}^{\gamma}(\text{HT}) \approx 3.12 \text{ \AA}^{-1}$ . Above  $T \approx 390$  K (HT state) the intensity of both peaks drops below LEED experimental sensitivity and only pseudomorphic diffraction spots remain. None of the widths of the diffraction peaks measured by LEED significantly changes upon reaching the high temperature regime. HeD data also show the  $\Gamma$  peak intensity decreasing with increasing temperature and the  $\Gamma$  peak position shifting to larger  $k_{\parallel}$ ; the He specular intensity increases drastically with temperature at  $T > 340$  K. The  $\Gamma$  peak

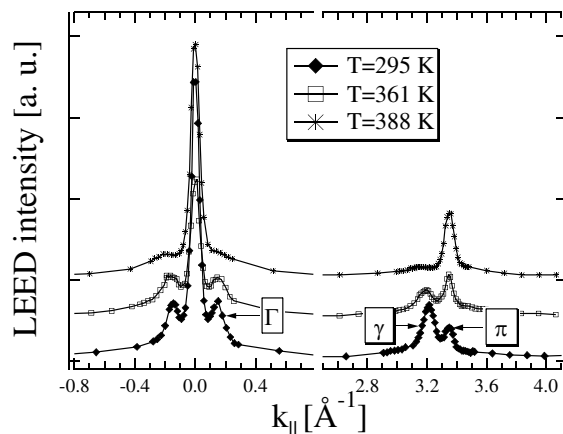


FIG. 1. Temperature dependent LEED line scans measured along (110) azimuth for 8 Å Fe/Cu<sub>3</sub>Au (see text for details).

remains observable by HeD up to a temperature of  $T \approx 395$  K, and its width increases above  $T \approx 360$  K. Temperature dependence of LEED peak intensities and positions are, respectively, reported in Figs. 2(a) and 2(b); HeD peak intensities and positions are shown in Figs. 2(c) and 2(b).

The most interesting observation is that, if the sample is cooled from  $T = 400$  K to RT, both  $\gamma$  and  $\Gamma$  peaks reversibly reappear, HeD specular intensity decreases, and at temperatures below  $T \approx 340$  K the initial situation is restored. Such a perfect reversibility is observed for a large number of thermal cycles, provided the sample is not heated above 400 K. We are therefore faced with a structural phase transition and clearly not with an irreversible temperature induced morphological rearrangement of the film. The transition is observable for both low temperature and RT deposited films. For the low temperature preparation, LEED diffraction peaks are sharp and well defined, and negligible Cu or Au intermixing within the film is observed, while RT deposition leads to a blurred LEED pattern, characterized by broader and weaker diffraction spots, and to the presence of Au intermixing within the film. LEED patterns recorded as a function of increasing thickness for both RT and 150 K deposited films reveal a gradual increase of the  $\gamma$  peak

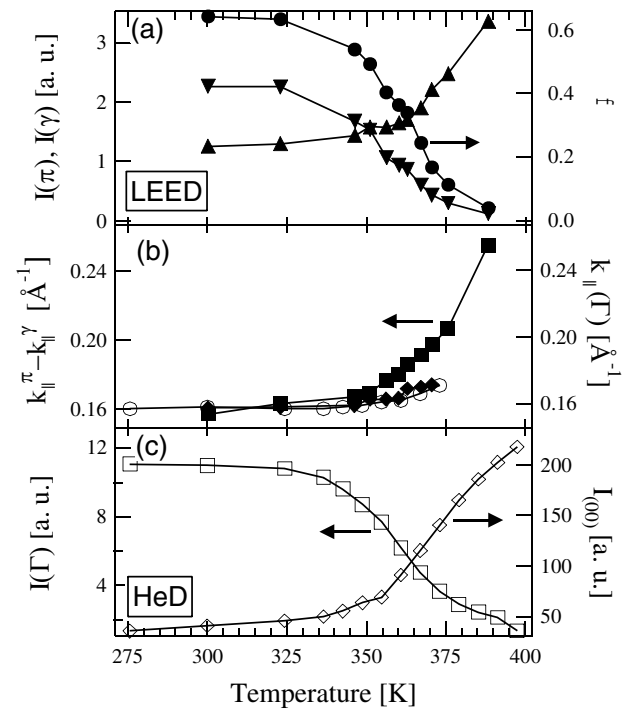


FIG. 2. Temperature dependence of HeD and LEED diffraction peak parameters for an annealed 8 Å Fe/Cu<sub>3</sub>Au film: open symbols refers to HeD data, and full symbols to LEED. (a)  $I_{\pi}$  (up triangles),  $I_{\gamma}$  (down triangles), and  $f = I_{\gamma}/(I_{\gamma} + I_{\pi})$  (circles) vs temperature. (b)  $k_{\parallel}(\Gamma)$  vs temperature measured by HeD (circles) and LEED (rhombi);  $(k_{\parallel}^{\pi} - k_{\parallel}^{\gamma})$  vs temperature (squares). (c) HeD specular (diamonds) and HeD  $\Gamma$  peak (squares) intensity vs temperature. Lines are guides to the eye.

contribution and corresponding decrease of the  $\pi$  peak. Above  $t \approx 12\text{--}13 \text{ \AA}$  coverage, detection of the  $\pi$  peak contribution can no longer be performed, indicative that all the topmost layers of the film possess  $\gamma$  structure. The in-plane periodicity of the  $\gamma$  phase in the LT state is observed to change slightly from measurement to measurement between  $2.78$  and  $2.74 \text{ \AA}$ , depending upon film thickness and fine details of the preparation procedure. The phase transition is observable within the  $6\text{--}11 \text{ \AA}$  Fe thickness range for films deposited at  $150 \text{ K}$  and in the narrower and upward shifted thickness range  $9\text{--}13 \text{ \AA}$  for RT evaporation. With increasing film thickness, we observe a slight monotonic increase of the transition temperature from  $T \approx 345 \text{ K}$  at  $6 \text{ \AA}$  to  $T \approx 380 \text{ K}$  at  $11 \text{ \AA}$  coverage (LT deposited films). At film thickness exceeding the limit of  $11$  and  $13 \text{ \AA}$  for LT and RT deposited films, respectively, the transition can no longer be observed, irrespective of the sample temperature.

The following discussion is aimed at understanding the structure of the  $\pi$  and  $\gamma$  phases and the driving forces of the transition. The HT phase of the film, combining evidence from HeD and LEED, appears to be fully pseudomorphic, smooth and ordered to a high degree, as deducible from the high intensity and narrow FWHM of HeD specular peak. The out-of-plane structure of the film, and particularly the value of the interlayer spacing  $h$  within the topmost Fe layers, can be extracted from HeD (00) beam rod scan analysis ( $I_{(00)}$  vs  $k_{\perp}$ , not shown). From these data the values of  $c = 2h$ , the out-of-plane size of the unit cell can be found, leading to straightforward calculation of  $c/a$ , the ratio of the out-of-plane to the in-plane sizes of the unit cell. For the low temperature preparation procedure, extrapolating HeD data to the whole film thickness, we obtain, for the pseudomorphic phase, a value of  $c/a$  of  $1.35 \pm 0.02$ , compatible with a ferromagnetic face centered tetragonal (fct) Fe structure [15], with volume per atom  $V_{\pi} = 12.6 \pm 0.2 \text{ \AA}^3$ . RT deposition gives a slightly larger value of  $c/a = 1.38 \pm 0.02$ , with volume per atom  $V_{\pi} = 12.8 \pm 0.2 \text{ \AA}^3$  likely stabilized by Au impurities [9].

The LT state appears to possess a more complicated structure. A LEED pattern qualitatively similar to the one that we observe—however, obtained for different film preparation procedures—has already been discussed in Refs. [7,8]. In our case, we can deduce from LEED data that, besides a certain amount of pseudomorphic phase, a fraction of the Fe film is occupied by a structural phase characterized by an in-plane lattice constant in the range  $2.74\text{--}2.78 \text{ \AA}$ , expanded with respect to the substrate ( $2.65 \text{ \AA}$ ). The superstructure peaks  $\Gamma$  are therefore due to the formation of a coincidence pattern whose period is given by the rephasing length of these two lattices, as demonstrated by the fulfilment of the  $k$ -space equality  $k_{\parallel}^{\Gamma} = k_{\parallel}^{\pi} - k_{\parallel}^{\gamma}$  below transition temperature. This coincidence pattern is accompanied by a significant corrugation

at the surface, as unambiguously demonstrated by the  $\Gamma$  peak in HeD data. Our films can be modeled either as a sandwich structure, with few monolayers (MLs) of pseudomorphic  $\pi$  phase in contact with the substrate and the topmost layers occupied by the expanded phase  $\gamma$ , or composed by adjacent patches of pseudomorphic  $\pi$  and  $\gamma$  phases (likely a mixture of both structures is present). Based on HeD rod scans and on previous determination of thin Fe/Cu<sub>3</sub>Au(001) film structure [9], we can deduce for the  $\gamma$  phase a  $c/a \sim 1.20 \pm 0.02$  (LT Fe deposition) or  $c/a \sim 1.22 \pm 0.02$  (RT Fe deposition), indicative of an fct structure, with volume per atom, respectively,  $V_{\gamma} = 12.4 \pm 0.2 \text{ \AA}^3$  and  $V_{\gamma} = 12.5 \pm 0.2 \text{ \AA}^3$ . We point out, however, that uncertainties deriving from the complicated morphology of the LT phase of the film might affect the  $\gamma$  phase volume determination.

Concerning the transition dynamics, the experimental data are consistent with the observation of a first order type phase transition. The  $\pi$  phase grows, in fact, with increasing temperature at the expenses of the  $\gamma$  phase, with  $\pi$  and  $\gamma$  phases coexisting at all temperatures below  $\sim 390 \text{ K}$ . The HT state of the system is characterized by the presence of an ordered  $\pi$  phase; extinction of the  $\Gamma$  peak is then a consequence of the disappearance of the corrugation induced by the  $\gamma$  phase. The increase with temperature of HeD specular reflected intensity is a clear sign of the flattening of the surface at HT, while the increase of the  $\Gamma$  peak FWHM observed by HeD above  $360 \text{ K}$  is attributed to the fragmentation and shrinking of the residual  $\gamma$  domains when disappearing at HT.

The driving mechanism of this phase transition can in principle be either of electronic (including magnetic) or structural origin. However, energy terms related to the magnetic state of the film, although appealing in principle, can be ruled out on the basis of *in situ* MOKE measurements, showing the absence of any measurable correlation between the magnetic properties of the film and the structural phase transition.

There can be an energy difference between the LT and HT states due to electron confinement energy  $\Delta E_c$  that cannot, in principle, be excluded for Fe/Cu<sub>3</sub>Au [16,17]. However, besides the difficulty to evaluate it due to the metal/metal character of the system, the relatively extended Fe thickness range for which the transition is observed rules out any electronic effect related to “magic” film thicknesses.

Let us then focus on structural effects. Because of the heteroepitaxial character of Fe/Cu<sub>3</sub>Au, elastic energy  $E_{el}$  is accumulated within the overlayer, which is proportional to the square of the deviation of the overlayer lattice constant from its equilibrium value [15]. At very low thickness ( $1\text{--}2$  MLs) the energy gain due to the perfect matching between the film and substrate lattices (chemical potential) overcomes the elastic energy due to the strain. The latter increases linearly with the film thickness up to a critical value where it must be released

through lattice relaxation, accompanied by misfit dislocations. At the critical thickness, an effective temperature dependence of  $E_{el}$  can be induced if the overlayer and the substrate possess different values of thermal expansion coefficient, a mechanism which was proposed to be the driving force underneath a structural transition between LT relaxed body centered tetragonal (bct) and HT strained fct pseudomorphic phases of Cu on Pd(100) [18]. In our case the  $\pi$  phase is under lateral compressive strain (and vertical expansion), while the  $\gamma$  phase has relaxed by lateral expansion (and vertical compression) and its strain is released through a network of misfit dislocations giving rise to the coincidence pattern around the (00) reflected peak (both HeD and LEED). Since the thermal expansion coefficient of the substrate ( $1.9 \times 10^{-5} \text{ K}^{-1}$ ) is 60% larger than that of the deposited film ( $1.2 \times 10^{-5} \text{ K}^{-1}$ , for bulk Fe), the lattice misfit between the  $\pi$  ( $a = 2.65$ ) and  $\gamma$  ( $a = 2.74\text{--}2.78$ ) phases is slightly reduced upon temperature increase; hence, the strained phase is energetically favored or, equivalently, the critical thickness is increased. The value of the transition temperature is then determined by the balance between strain energy, the absolute energy of the  $\gamma$  and  $\pi$  phases, and the energy accumulated by the interfaces between pseudomorphic and nonpseudomorphic phases. The transition temperature shifts with thickness due to the corresponding shift of balance between the occupation of the film by  $\pi$  and  $\gamma$  phases. The upper thickness limit of the transition can be set by the formation of a thick and stable slab of the  $\gamma$  phase on top of the film, effectively inhibiting enlargement of  $\pi$  phase patches. The shift of the  $\gamma$  peak towards smaller  $k_{\parallel}$  values can be explained bearing in mind that it represents a statistical distribution of  $\gamma$  domains with slightly different misfits. As the  $\pi$  phase domains grow upon temperature increase, the transformation of  $\gamma$  domains by lateral compression starts from those with the smallest misfit. Thus the residual  $\gamma$  peak at the critical temperature simply represents the low  $k_{\parallel}$  tail of the misfit statistical distribution of  $\gamma$  domains; i.e., the last  $\gamma$  domains to transform are those with the largest misfit. In this nondiffusive picture of the phase transition, the pair correlation among the  $\gamma$  domains is not expected to change while disappearing, as witnessed by the  $\Gamma$  peak behavior, whose shift is negligible with respect to the  $\gamma$  peak one and only broadens at its disappearance. According to the above discussion, in order to observe a reversible pseudomorphism breakdown transition, a given substrate and overlayer must show large differences in thermal expansion coefficients, the growth of the overlayer must be epitaxial, and the overlayer structure must possess two energy minima as a function of its lattice constant. Furthermore, the value of the substrate lattice constant must be close to the epitaxial unstable region between such minima [19], so that a small temperature induced lattice constant variation can have a large effect

on the overlayer structure. In the Fe/Cu(001) case, despite the large amount of experimental investigations, no such behavior was reported. Thus, a suitable system should have a lattice constant and a thermal expansion coefficient larger than Cu ones ( $2.55 \text{ \AA}$  and  $1.65 \times 10^{-5} \text{ K}^{-1}$ , respectively). As a consequence, among the pure elements where thin fcc Fe films can be grown, we must exclude Rh, Pd, and Pt, since they fulfill the requirement on lattice constant, but have a thermal expansion coefficient lower than the Fe one. Excluding Au (whose lattice constant is slightly larger than the Fe bcc one), the only pure element left is Ag. Its thermal expansion coefficient,  $1.89 \times 10^{-5} \text{ K}^{-1}$ , is close to the  $\text{Cu}_3\text{Au}$  one; however, its lattice constant,  $2.84 \text{ \AA}$ , is possibly too large and this system undergoes a more complex irreversible transformation upon film annealing [20]. The only route left seems to be the fabrication of a suitable alloy for achieving a fine control of the lattice constant and thermal expansion coefficient.

In summary, we have shown that ultrathin Fe/ $\text{Cu}_3\text{Au}$  films within a critical thickness range, which is beyond pseudomorphism breakdown thickness at RT, undergo a temperature dependent structural phase transition at  $T \sim 360 \text{ K}$ . Above this temperature full pseudomorphism is observed, while pseudomorphism breakdown reversibly takes place as the system is cooled below transition temperature.

The authors acknowledge Professor G. Boato, D. Cvetko, W. Hofer, D. Alf e, and the late Paolo Cantini for stimulating discussions.

---

\*Electronic address: Bisio@fisica.unige.it

- [1] S. H. Lu *et al.*, Surf. Sci. **209**, 364 (1989).
- [2] J. Thomassen *et al.*, Phys. Rev. Lett. **69**, 3831 (1992).
- [3] M. Wuttig and J. Thomassen, Surf. Sci. **282**, 237 (1993).
- [4] J. Giergiel *et al.*, Phys. Rev. B **52**, 8528 (1995).
- [5] M. Zharnikov *et al.*, Phys. Rev. Lett. **76**, 4620 (1996).
- [6] A. Biedermann *et al.*, Phys. Rev. Lett. **87**, 086103 (2001).
- [7] B. Feldmann *et al.*, Phys. Rev. B **57**, 1014 (1998).
- [8] B. Schirmer, B. Feldmann, and M. Wuttig, Phys. Rev. B **58**, 4984 (1998).
- [9] F. Bruno *et al.*, Phys. Rev. B **66**, 045402 (2002).
- [10] V. L. Moruzzi *et al.*, Phys. Rev. B **34**, 1784 (1986).
- [11] V. L. Moruzzi, P. M. Marcus, and J. K ubler, Phys. Rev. B **39**, 6957 (1989).
- [12] P. M. Marcus, V. L. Moruzzi, and S. -L. Qiu, Phys. Rev. B **60**, 369 (1999).
- [13] C. Mannori *et al.*, Europhys. Lett. **45**, 686 (1999).
- [14] F. Bisio *et al.*, Appl. Surf. Sci. **212–213**, 166 (2003).
- [15] P. M. Marcus and F. Jona, Surf. Rev. Lett. **1**, 15 (1994).
- [16] M. Canepa *et al.*, Phys. Rev. B **62**, 13121 (2000).
- [17] A. Verdini *et al.*, Phys. Rev. B **65**, 233403 (2002).
- [18] E. Hahn *et al.*, Phys. Rev. Lett. **74**, 1803 (1995).
- [19] P. Alippi *et al.*, Phys. Rev. Lett. **78**, 3892 (1997).
- [20] S. Terreni *et al.*, cond-mat/0401142.